

OMAE2011-49262

CANCELLATION OF NON-HARMONIC WAVES USING A CYCLOIDAL TURBINE

John T. Imamura

Department of Aeronautics
United States Air Force Academy
Air Force Academy, Colorado 80840
Email: john.imamura@usafa.edu

Stefan G. Siegel

Department of Aeronautics
United States Air Force Academy
Air Force Academy, Colorado 80840
Email: stefan@siegels.us

Casey Fagley

Department of Aeronautics
United States Air Force Academy
Air Force Academy, Colorado 80840

Tom McLaughlin

Department of Aeronautics
United States Air Force Academy
Air Force Academy, Colorado 80840

ABSTRACT

We computationally investigate the ability of a cycloidal turbine to cancel two-dimensional non-harmonic waves in deep water. A cycloidal turbine employs the same geometry as the well established Cycloidal or Voith-Schneider Propeller. It consists of a shaft and one or more hydrofoils that are attached eccentrically to the main shaft and can be independently adjusted in pitch angle as the cycloidal turbine rotates. We simulate the cycloidal turbine interaction with incoming waves by viewing the turbine as a wave generator superimposed with the incoming flow. The generated waves ideally are 180° out of phase and cancel the incoming wave downstream of the turbine. The upstream wave is very small as generation of single-sided waves is a characteristic of the cycloidal turbine as has been shown in prior work. The superposition of the incoming wave and generated wave is investigated in the far-field and we model the hydrofoil as a point vortex. This model has previously been used to successfully terminate regular deep water waves as well as intermediate depth water waves. We explore the ability of this model to cancel non-harmonic waves. Near complete cancellation is possible for a non-harmonic wave with components designed to match those

generated by the cycloidal turbine for specified parameters. Cancellation of a specific wave component of a multi-component system is also shown. Also, step changes in the device operating parameters of circulation strength, rotation rate, and submergence depth are explored to give insight to the cycloidal turbine response characteristics and adaptability to changes in incoming waves. Based on these studies a linear, time-invariant (LTI) model is developed which captures the steady state wave frequency response. Such a model can be used for control development in future efforts to efficiently cancel more complex incoming waves.

NOMENCLATURE

T Wave Period [s]
 D Water Depth [m]
 H Wave Height [m]
 C Wave Travel Velocity (Celerity) [m/s]
 C_g Wave Group Velocity [m/s]
 k Wave Number [1/m]
 g Gravity constant, $9.81[\text{m/s}^2]$

- t Time [s]
- λ Wavelength [m]
- R Wave Energy Converter Radius [m]
- x_c, y_c Wave Energy Converter Shaft location [m]
- ϕ Flow Potential [m^2/s]
- η Water Surface [m]
- Γ Vortex or Hydrofoil Circulation [m^2/s]
- $\delta(t)$ Main Shaft rotational angle [deg]
- θ Feedback phase [deg]
- $F(z, t) = \phi + i\psi$ Complex Stream Function
- σ Phase angle

INTRODUCTION

Ocean wave energy is one of the most abundant sources of renewable energy on Earth. The field of ocean wave energy extraction has gained considerable interest within the past several years due to the increasing need for greater renewable energy generation. Various device designs exist which attempt to harness this energy. These devices generally rely on water pressure acting over large surface areas to cause relative motion within the design from which the power is derived. The cycloidal turbine wave energy extraction concept on the other hand interacts with waves by using lift. This device design consists of a main shaft capped at the ends by two discs. One or more hydrofoils attached eccentrically from the main shaft by the discs and can be adjusted independently in pitch angle. The whole device is submerged in the water and oriented such that the main shaft aligns with the crests of incoming waves as seen in Figure 1. The hydrofoils act as wings moving through the wave velocity field at orbital motion speeds and hence can generate large forces for a comparatively small size [1].

The concept of the cycloidal turbine wave energy converter

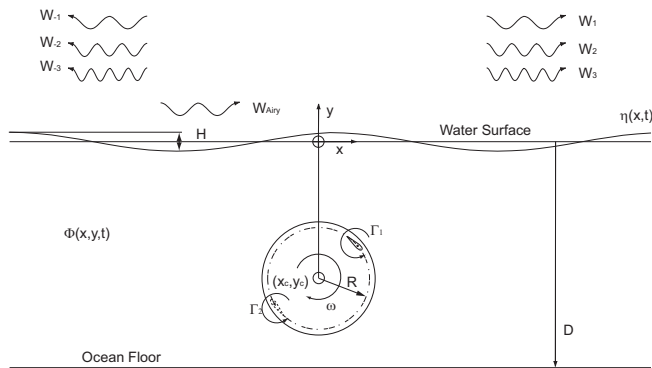


FIGURE 1. Cycloidal wave energy converter geometry.

is to synchronize rotation of the device to the frequency of the

incoming waves. When synchronization occurs the flow around the hydrofoil generates a lift force on the hydrofoils and that force produces a torque which continues the rotation. Early initial work in this area was carried out at TU Delft by Hermans, van Sabben, and Pinkster [2]. They carried out experiments using a single hydrofoil ‘rotating wing’ attached to a submerged horizontal shaft. Testing in regular waves showed that weights could be lifted by using the rotating shaft as a winch. Their work also developed a theory to model the generation of waves by this device based on two-dimensional linear potential theory. An important conclusion was that waves are generated “down stream” only. The direction of the generated waves corresponds with the direction of motion of the foil when at the highest point of its rotation [3].

More recently computational and experimental work has been done at the US Air Force Academy to further characterize the wave generation from a rotating hydrofoil. Computational work to explore the use of the cycloidal turbine as a wave generator as well as a wave terminator has been conducted [4, 5]. As expected, single-sided waves were generated and the wave direction was controlled by the hydrofoil rotation direction. The frequency of the generated wave matched the rotation frequency of the cycloidal turbine. Also as expected was a linear increase in wave amplitude with circulation strength. Physically, circulation strength is related to the pitch angle of the hydrofoils. Wave amplitude also increased with a reduction in submergence depth, though the effect was not proportional and varied between the various generated wave components.

In general the generated waves were composed of up to three components, a fundamental Airy type wave and its first two harmonics. A parameter study of wave energy converter size was conducted to investigate these components. This study gives guidance for the amplitude of wave components generated at a given device radius for a desired generated fundamental wavelength. A typical result from [4] is shown in Figure 2 for a nine second period. For a wide range of device sizes the fundamental wave is dominant, however for small values of non-dimensional device size the first and second harmonics contribute more significantly to the generated wave. One conclusion of the study was a peak in fundamental wave amplitude occurs at $2R/\lambda_{Airy} = 1/\pi$. Another interesting conclusion was on the effect of using two hydrofoils of opposite circulation and placed 180° apart. Cancellation of the first harmonic wave was shown to result. This is a useful device configuration to generate near sinusoidal waves.

Wave cancellation or termination of deep water and intermediate water waves [5] has been simulated quite successfully for regular waves. The single-sided wave generation feature of the cycloidal turbine is well suited for this task. Achieving cancellation requires the motion of the cycloidal turbine to be synchronized in frequency and phase locked to the incoming wave. The circulation of the hydrofoils must be adjusted to

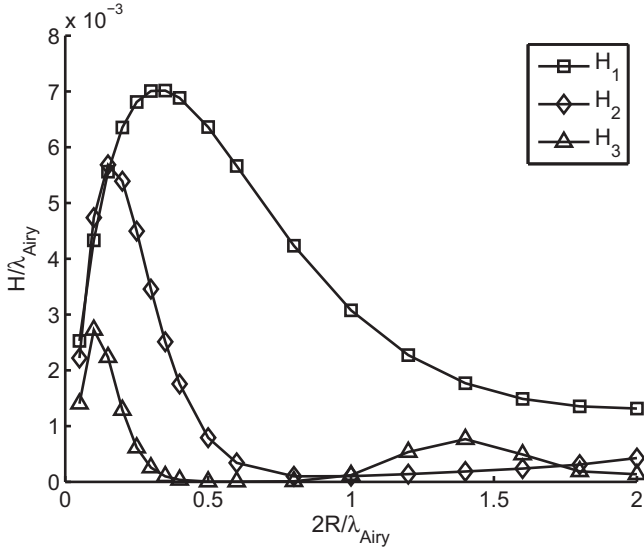


FIGURE 2. Wave height for different sizes $2R/\lambda$ of the cycloidal turbine located at $(y_c - R)/\lambda = 0.03$. All waves evaluated at $+3\lambda$ at $t/T = 30$ for a $T = 9s$ wave [4].

produce the same wave amplitude as the incoming wave. The superposition of the two waves results in a flat water surface downstream of the cycloidal turbine. The modeling in the referenced works utilizes potential theory and assumes the cycloidal turbine does not impede the incoming wave. In this work we utilize the same model and assumptions to explore wave cancellation for non-harmonic waves.

Real ocean waves are more complex than simple regular waves of course. They can usually be described as having random wave heights and composed of many frequencies. Non-harmonic waves considered for this work will be superpositions of multiple sinusoidal waves. We show that with knowledge of the incoming wave components some portion of the wave can be terminated by the cycloidal turbine. We also explore how step changes to the device parameters affects the generated wave. These results show how responsive the cycloidal turbine can be to changes in the incoming wave. Results to step changes can serve as building blocks for future work on a comprehensive wave estimation and feedback control scheme for cancelling and ultimately extracting energy efficiently from real ocean waves.

COMPUTATIONS

Mathematical Formulation

We apply linear potential theory to solve for the water surface generated by the rotating hydrofoils. We assume incompressible, inviscid flow in infinite depth water. The fluid velocity

is described by the velocity potential $\phi(x, y, t)$ as

$$\bar{u} = \nabla\phi \quad (1)$$

The field equation becomes

$$\nabla^2\phi = 0 \quad (2)$$

and allows for superposition. At the linearized free surface we combine the kinematic and dynamic free surface boundary equations to get

$$\frac{\partial^2\phi}{\partial t^2} + g\frac{\partial\phi}{\partial y} = 0 \quad (3)$$

The free surface elevation $\eta(x, t)$ is given by

$$\eta = -g\frac{\partial\phi}{\partial t} \quad (4)$$

The potential for a vortex moving under a free surface which satisfies the conditions above is given by Wehausen and Laitone [6]

$$F(z, t) = \frac{\Gamma(t)}{2\pi i} \ln\left(\frac{z - c(t)}{z - \bar{c}(t)}\right) + \frac{g}{\pi i} \int_0^t \int_0^\infty \frac{\Gamma(\tau)}{\sqrt{gk}} e^{-ik(z - \bar{c}(\tau))} \sin\left[\sqrt{gk}(t - \tau)\right] dk d\tau \quad (5)$$

where $c(t)$ is the vortex position in the complex plane, $\bar{c}(t)$ is the complex conjugate, $\Gamma(t)$ is the vortex circulation, g is gravity, and k is wave number.

This potential is solved for using the same second order spatial and time marching techniques as in Siegel et. al. [4,5]. Based on their numerical resolution study, convergence is achieved for the following values of wave number increment, maximum wave number, and time discretization increment: $k/\Delta k = 31.6$, $k_{max}/k = 75.9$, and $T/\Delta t = 36$. These values have been used for the results in this work. In addition this numerical method has been compared to the work of the TU Delft group [2] and good agreement was found between this method and their analytical and experimental results.

As discussed earlier, the non-harmonic waves considered in this work are superpositions of regular waves with differing amplitudes, frequencies, phase angles. Therefore the incoming wave surface is described as

$$\eta_{incoming} = \sum_i A_i \sin(\omega_i t + \sigma_i) \quad (6)$$

Wave Energy Converter Motion

The positions of the vortices are prescribed in this work. We determine the vortices' position through control of the cycloidal turbine rotation rate and the submergence level. For all cases the location of the cycloidal turbine is fixed in the x direction. The location of the main shaft (center of rotation of the vortices) is denoted y_c as shown in Figure 1. The level of submergence is controlled by this parameter. Therefore the coordinates of the vortex moving with radius R and angular frequency ω_c are

$$c_x(t) = R \cos(\omega_c t + \theta) \quad (7)$$

$$c_y(t) = y_c - R \sin(\omega_c t + \theta) \quad (8)$$

Here θ is a phase shift that can be used to synchronize the incoming wave and the frequency of the cycloidal turbine.

RESULTS

In this section results will be presented with a focus on nine second period waves. The motivation for this is that the North Atlantic often features waves of this period [7], so this is useful from a design perspective. This approach also allows us to utilize results from the prior cited works by Siegel et.al.

Inverse Problem

As described in past wave generation studies by Siegel et. al. [4, 5] Fast Fourier Transform analysis has been performed to obtain the wave component amplitudes and frequencies. Using this technique we can analyze the steady state portion of any generated wave. From this information we can construct an incoming inverse wave correctly phase shifted to the generated wave. Figure 3 demonstrates this process. The top plot shows the free surface time history at three wavelengths downstream created by a single vortex. The middle plot shows the constructed input wave. As shown on the bottom of the figure the superposition of these two waves results in near complete wave cancellation once the generated wave reaches steady state.

Cancellation of a Wave Component

Next we show cancellation of one component of an incoming multi-component wave system. For these runs we have chosen cycloidal turbine parameters of $2R/\lambda_{Airy} = 0.75$ and $y_c/\lambda_{Airy} = 0.405$ and used two vortices of equal but opposite circulation placed 180° apart to generate a nearly sinusoidal nine second, steady state wave. As indicated in Figure 2 only very small harmonic waves are generated in addition to the fundamental wave for this value of non-dimensional radius. Likewise at this level of submergence depth harmonic waves are minimal. Figure 4 demonstrates this type of cancellation. The top plot

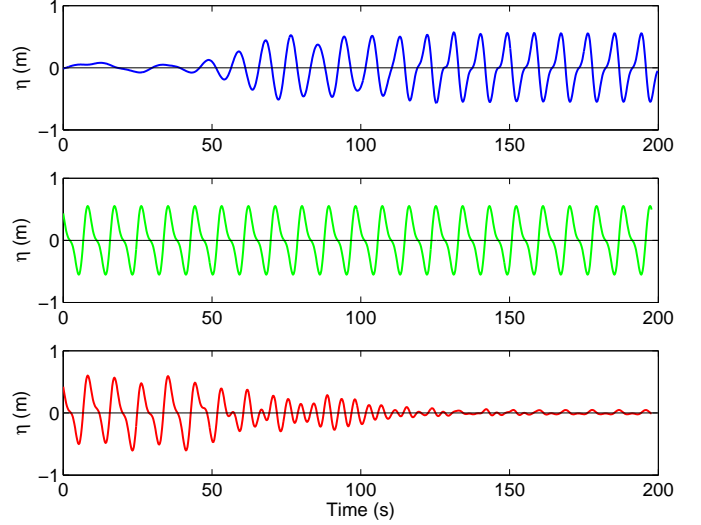


FIGURE 3. Water surface time histories at $x = +3\lambda$, $R = 20.203m$, $y_c = -24m$, $\Gamma = 10m^2/s$, single vortex wave generation. (Top) Wave generated of 9 second fundamental period. (Middle) Incoming non-harmonic wave. (Bottom) Resulting wave.

shows the expected sinusoidal 9 second period generated wave. The middle plot shows the 9 and 9.9 second period waves which combine to make up the two-component incoming wave. The bottom plot shows the resulting superposition of the generated and incoming wave. Clearly the steady state portion matches that of the 9.9 second period wave from the middle plot indicating the 9 second wave has been cancelled. We performed many similar test cases combining a nine second period wave with wave periods between five and 13 seconds. As expected from a model utilizing superposition we are able to successfully cancel the nine second wave in all cases. Similarly, superposition allows us to extrapolate this cancellation of the nine second wave to wave systems of any number of waves. In these cases the phase shift between the generated wave and the wave component to cancel were known in advance.

Response to Change in Cycloidal Turbine Parameters

The above results showed successful wave cancellation for periodic waves. However, in all likelihood the wave conditions will change in time requiring a change in the device parameters to maintain synchronicity. The response of generated waves to changes in device parameters is unknown. Thus, in this section we will explore the behavior of the downstream generated waves to step changes in the device parameters. This investigation will give insight to the responsiveness of the cycloidal turbine. The waves generated in this section were all created using the two vortices configuration.

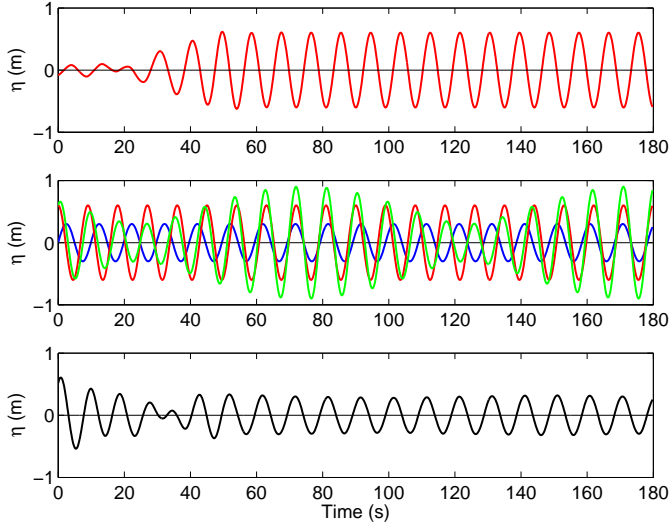


FIGURE 4. Water surface time histories at $x = +2\lambda$, $R = 47.4375m$, $y_c = -51.2325m$, $\Gamma = \pm 10m^2/s$, double vortex wave generation. (Top) Sinusoidal generated wave of 9 second period. (Middle) Two component wave (green) composed of a 9 second period wave (red) and a 9.9 second period wave (blue). (Bottom) Resulting wave where the 9 second period wave is cancelled out.

Step Change in Circulation The circulation strength, Γ is directly related to the generated wave height. Thus we expect this to be a useful control parameter when adapting to changing incoming wave amplitudes. In Figure 5 we look at the response of a nine second period ($T = 9s$) generated wave to a step change in the circulation strength. Two results are shown, one for an increase in Γ and one for a decrease. In both cases the step change occurred after 10 periods (at 90 seconds). As expected the increase and decrease in the steady state wave amplitude is proportional to the change in Γ . It is also of interest to note the time duration to achieve a steady state after the step change occurs. The presented results are the water surface time history at two wavelengths downstream. It appears from the figure that the transient behavior lasts for approximately 50 to 60 seconds (~ 6 periods). If a perfect change in wave amplitude were to occur the step change in amplitude would occur after a propagation time of 18 seconds (2 periods). Thus approximately 4 periods are required to develop a steady state wave following a step change in Γ for a 9 second period wave.

Step Change in Submergence The level of submergence is another parameter that can be used to control the amplitude of the generated wave. Like with the circulation strength parameter, we investigated the response of a nine second period generated wave to a step change in the level of submergence. This is shown in Figure 6. Two plots are displayed for the water

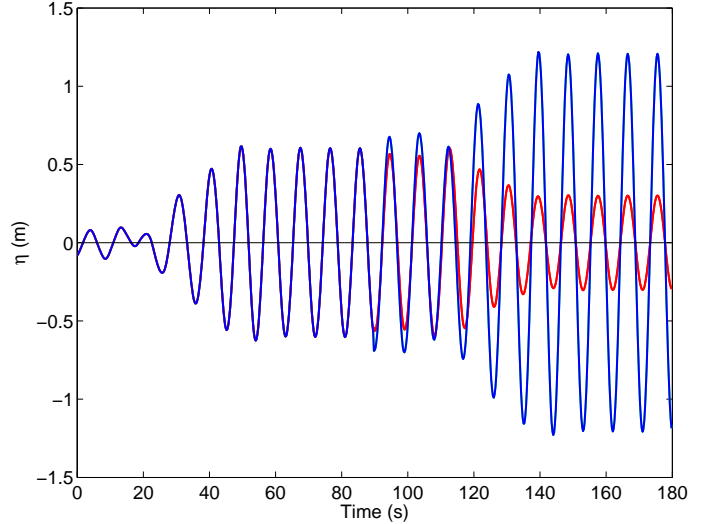


FIGURE 5. Water surface time histories at $x = +2\lambda$, $R = 47.4375m$, $y_c = -51.2325m$, double vortex wave generation. Step change in circulation from $\Gamma = \pm 10m^2/s$ to $\Gamma = \pm 20m^2/s$ at $t = 90s$ (in blue). Step change in circulation from $\Gamma = \pm 10m^2/s$ to $\Gamma = \pm 5m^2/s$ at $t = 90s$ (in red).

surface time history two wavelengths downstream over 20 periods. Γ and rotation rate are fixed for both cases. The step change occurs after 10 periods (at 90 seconds). The plot in red is for a step change increase in the level of submergence and shows the expected decrease in steady state wave amplitude. The blue plotted line is for a step change reduction in the submergence level and shows the expected increase in steady state wave amplitude. In both cases approximately 50 to 60 seconds (~ 6 periods) are required before the generated wave returns to steady state. As was the case for the step change in circulation runs, 18 seconds (2 periods) are required for propagation time so approximately 4 periods are required to develop a steady state following a step change in submergence.

A parameter study was also conducted to determine the generated wave amplitude dependence on the level of submergence. Figure 7 shows these results of increasing the submergence to up to twice the initial submergence. The dependence is non-linear. The dependence shows lowering the cycloidal turbine reduces the generated wave height and the reduction decreases with greater submergence. For the parameters chosen, the generated wave height is reduced to 20% of the initial wave height for a doubling of the submergence.

Step Change in Period We now consider a step change in the period of wave generated or equivalently the frequency of rotation of the cycloidal turbine. This parameter allows us to adapt the cycloidal turbine to account for changes in the incoming wave frequency. For the results presented here we con-

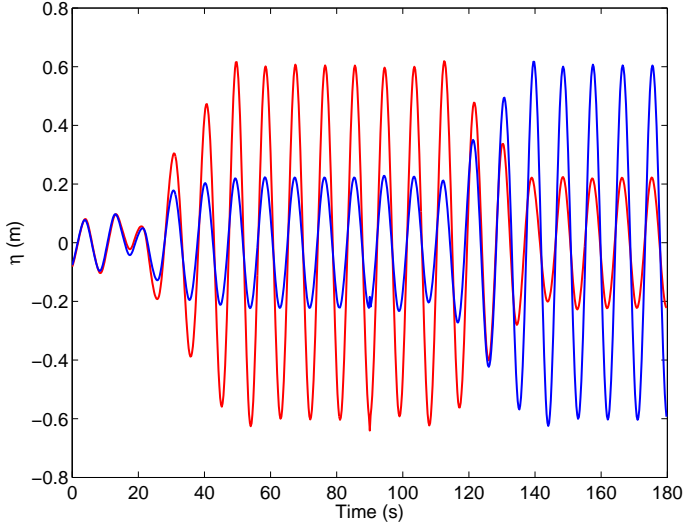


FIGURE 6. Water surface time histories at $x = +2\lambda$, $R = 47.4375m$, $\Gamma = \pm 10m^2/s$, double vortex wave generation. Step change in submergence from $y_c = -51.2326m$ to $y_c = -76.8487m$ (red). Step change in submergence from $y_c = -76.8487m$ to $y_c = -51.2326m$ (blue).

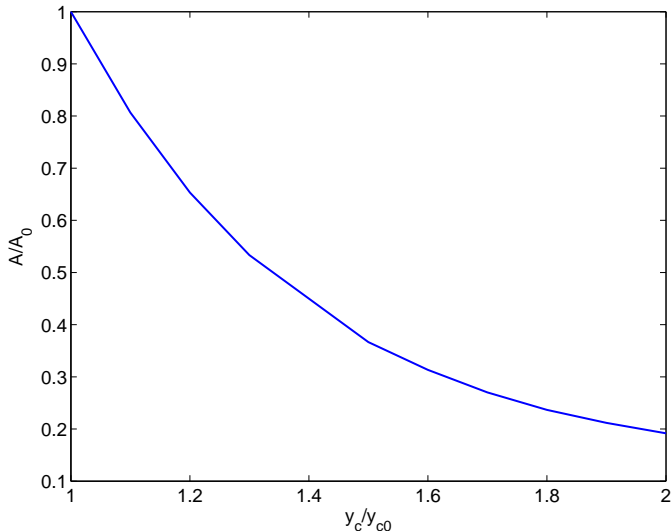


FIGURE 7. Generated wave amplitude for varying submergence. Cycloidal turbine parameters are $T = 9s$, $R = 47.4375m$, $\Gamma = \pm 10m^2/s$, double vortex wave generation. Max generated wave amplitude $A_0 = 0.6m$ for initial submergence level of $y_{c0} = -51.2325m$.

sider constant circulation ($\Gamma = \pm 10m^2/s$), constant submergence ($y_c = -51.2325m$), and an initial wave generation time of 10 periods. The generated wave height data is recorded at two wavelengths (of a 9 second wave) downstream. For this study we looked at step change between a 9 second period to a 6, 7, 8, 10, 11, 12, or 13 second period and vice versa. A select representative set of results are presented here.

Consider an initial wave of 9 second period. Steady state is reached after ~ 50 seconds of the startup transients with an amplitude of $0.60m$. After 10 periods (at 90 seconds) the rotation rate is step changed to produce either 6 or 13 second periods. The results are presented in Figure 8. For the case of changing to 6 second periods the wave appears to reach a steady state amplitude of $0.07m$ after a transient time of 60 seconds. For the case of changing to 13 second periods the wave appears to reach a steady state amplitude of $0.72m$ after a transient time of ~ 60 to 70 seconds. After the transient period the waves generated

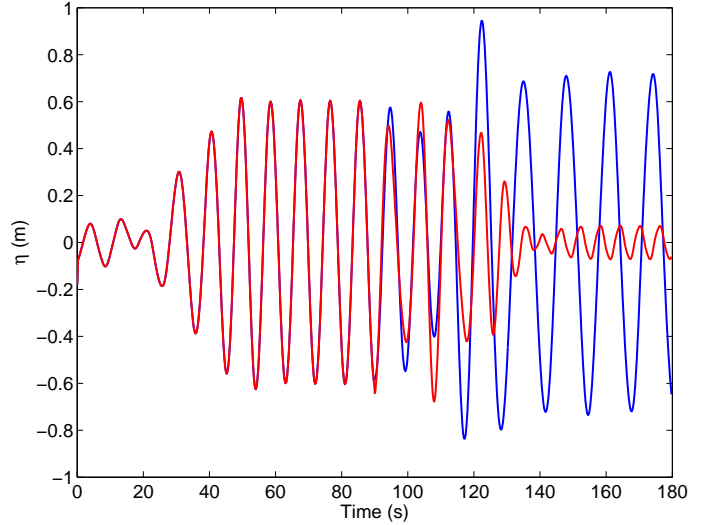


FIGURE 8. Water surface time histories at $x = +2\lambda$, $R = 47.4375m$, $y_c = -51.2325m$, $\Gamma = \pm 10m^2/s$, double vortex wave generation. Step change in period from $T = 9s$ to $T = 13s$ (blue) at $t = 90s$. Step change in period from $T = 9s$ to $T = 6s$ (red) at $t = 90s$.

clearly return to near sinusoids with periods of 6 and 13 seconds.

Now consider initial waves of 6 and 13 second periods. After 10 periods, the rotation rate is changed to produce a 9 second period. These results are presented in Figure 9. The red line shows the initial 6 second wave reaches a steady state amplitude of $0.07m$ after a transient period of between 50 to 60 seconds. The step change occurs at 60 seconds and following an approximately 50 second transient the 9 second, $0.6m$ amplitude steady state wave is reached. For the case of the 13 second initial period wave (in blue) the steady state amplitude of $0.72m$ is reached after ~ 60 to 70 seconds. The step change occurs at 130 seconds and again after approximately 50 seconds of transient time the wave tends toward a 9 second, $0.6m$ amplitude steady state.

Transient Time and Steady State Amplitude Dependence on Period Transients in the generated wave occur during the initial wave generation startup and after the step change.

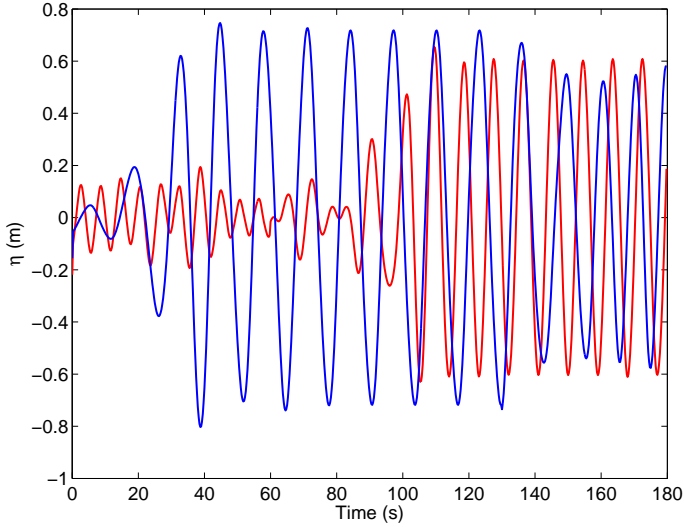


FIGURE 9. Water surface time histories at $x = +2\lambda$, $R = 47.4375m$, $y_c = -51.2325m$, $\Gamma = \pm 10m^2/s$, double vortex wave generation. Step change in period from $T = 13s$ to $T = 9s$ (blue) at $t = 130s$. Step change in period from $T = 6s$ to $T = 9s$ (red) at $t = 60s$.

A comparison of these two types of transients for the step change in period runs show they are similar in duration. These transient times are shown in Table 1. These times are given as a range because it is unclear at what point between wave peaks that the transients end and steady state begins. In all cases the water surface data was taken at $x = 253m$ corresponding to two wavelengths downstream for a 9 second wave. The values presented in the table are the duration of the transient after taking into account the propagation time of the generated waves. The propagation time is assumed to be $253m/celerity$ where celerity is the deepwater wave speed for the given wave period. The results show that in general 4 to 5 periods are required following a step change in the period before steady state is achieved.

Model Formulation

The open loop simulations are a necessary means to developing a model which accurately captures the steady state frequency response of the cycloidal turbine. Determining the model structure (ie linear/non-linear, first/second order, time varying/invariant, etc.) is the initial step. It is seen by Figure 5 that the cycloidal turbine is linear in prescribed circulation to output wave height at a given frequency; also, Figures 8-9 show a non-linear relation in generated wave height and frequency. Thus a linear time invariant model (LTI) is a wise choice. If the input $u(t)$ is defined as the prescribed circulation of the single point vortex and the output $y(t)$ is defined as the measured wave height at a given location, a LTI black box model is well representative of the cycloidal turbine at a given operating condition. For ex-

TABLE 1. Wave Generation Properties for $R = 47.4375m$ and $y_c = -51.2325m$, and transient durations (after accounting for propagation time).

Gen. Wave		Transient Time		
T(s)	Amp(m)	Startup(s)	Step Change(s)	Periods(T)
6	0.07	23 to 33	23 to 33	~3.8 to 4.7
7	0.15	42 to 47	32 to 37	~4.6 to 6.7
8	0.30	45 to 50	40 to 50	~5.0 to 6.3
9	0.60	32 to 42	37 to 47	~3.6 to 5.2
10	0.60	49 to 59	44 to 49	~4.4 to 5.9
11	0.61	55 to 65	50 to 60	~4.5 to 5.9
12	0.70	56 to 66	51 to 61	~4.3 to 5.5
13	0.72	53 to 63	58 to 68	~4.1 to 5.2

ample if the input has form,

$$u(t) = \Gamma \sin(\omega t),$$

then for a LTI system the output will take the form

$$y(t) = \lambda(\omega) \sin(\omega t + \theta(\omega)).$$

Typically linear systems are better represented in the Laplace domain as,

$$Y(s) = \frac{b_0 + b_1s + \dots + s^m}{a_0 + a_1s + \dots + a_n s^n} U(s) = G(s)U(s).$$

The gain and phase of the transfer function ($G(s)$) are then defined as $|G(j\omega)| = \frac{\lambda(\omega)}{\Gamma}$ and $\angle G(j\omega) = \theta(\omega)$, respectively. Identifying the parameters of the transfer function ($b_0 \dots b_m$, and $a_0 \dots a_n$) is a challenging process. The unit step response is a powerful tool to identify such transfer functions. The step response can help to predict model order and damping of the unknown system. Figure 5 shows that a step change from an initial state to a new state indicates an over damped system. To model the magnitude of generated wave over the range of frequencies a bode plot is generated to better understand the data, shown in Figure 10. Here the magnitude is presented in terms of decibels, $20 \log_{10} \left(\frac{\lambda(\omega)}{\Gamma} \right)$. Typical system identification methods may be

used to model the frequency domain data. In particular, the prediction error method gives a nice iterative scheme to solve for the transfer function $G(s)$. The cost function is minimized in a mean square sense, such that

$$J_N(B, A) = \sum e^2(t),$$

where the error is defined as

$$e(t) = y(t) - \hat{y}(t) = y(t) - A^{-1}(q)B(q)u(t),$$

given a parameter structure for the numerator and denominator for the difference equation. The model output and simulated Airy wave data are shown in Figure 10. The specific identified model is,

$$G(s) = \frac{0.0022s^4 - 0.1962s^3 + 0.0060s^2 - 0.1330s + 0.0062}{s^5 + 0.0077s^4 + 0.4775s^3 - 0.0011s^2 - 0.1141s + 0.0066}$$

Note, these are only initial model identification attempts; further iteration needs to be done on model order and parameter selection. Nonetheless a linear, fifth order model does represent the steady state simulation data well.

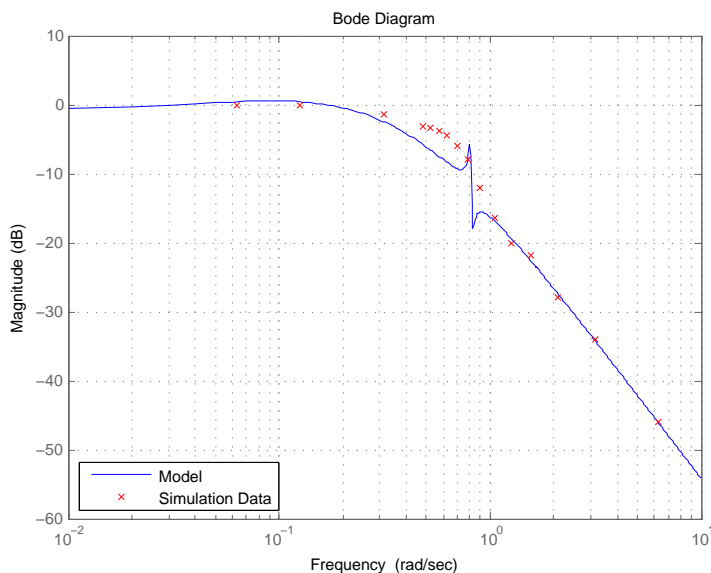


FIGURE 10. Frequency vs magnitude plot of simulated steady state data (red). Fifth order Prediction Error Method model.

The developed linear model can then be utilized for control development. Typical control design methods such as: loop shaping techniques, PID, H_∞ , model predictive control, μ -synthesis, etc. may be used to control the rotational frequency and circulation (equivalently Angle of Attack) to produce a desired wave height and frequency. This control effort will eventually be invoked to cancel completely unknown periodic waves. Also, it is shown by Figure 7 that a non-linear relation between submergence depth and generated wave height exist. A series of linear models at each operating point (submergence depth) will need to be employed to span the entire parameter space.

DISCUSSION AND SUMMARY

The results of this research show that cancellation of all or part of incoming non-harmonic waves is possible by using a cycloidal turbine as a wave generator. The generation of the ‘anti’ wave (of matching amplitude and out of phase by 180°) necessary for cancellation requires knowledge of the incoming wave amplitude and phase. For incoming periodic waves which match the characteristics of waves the cycloidal turbine can produce, near complete cancellation is possible as was shown for the inverse problem. The ability of the cycloidal turbine to generate sinusoidal waves is very useful in cancelling wave components of multi-component wave systems. Through superposition of the generated wave with the incoming wave, a desired wave component can be cancelled.

We next considered wave generation in response to step changes in the cycloidal turbine operating parameters. This was done to gain insight to the response characteristics of the device to changes in the incoming waves. A consistent result in all the step change runs was a transient time of approximately 4 to 6 periods. This result holds over the range of periods from 6 to 13 seconds which we considered and regardless of whether the change occurred at startup or after a steady state was achieved. A possible explanation for this transient time is simply that this number of periods is required to produce a periodic wave. If we consider the step change to a cycloidal turbine parameter as a disturbance to the flow, one can expect a multitude of waves to be generated. After a couple rotations following the step change all the generated waves not in sync to the rotation period cancel out leaving only the propagating periodic wave. Observational evidence of wavemakers support this notion that steady wavetrains require several periods to develop. A logical conclusion that can be drawn is that this places a lower limit to achieve a new steady state for a control algorithm responding to changes in the incoming waves.

Results were also presented for the generated wave response to step changes in the cycloidal turbine parameters of circulation strength, period, and submergence. These step change investigations give insight to how the cycloidal turbine parameters need to be changed in response to changing incoming wave conditions.

Both the circulation strength and submergence parameters can be used to change the generated wave amplitude to match that of the incoming wave. In the case of circulation strength there is a linear relationship to the steady state wave amplitude, while the relationship is non-linear for submergence. For both cases a transient time of approximately four periods follow the step change before the generated wave returns to steady state. The period of the generated wave can also be changed by changing the rotation rate of the cycloidal turbine. Once again a new steady state wave followed a transient time of approximately four periods. In the step change runs to change period, the resulting steady state amplitude also changed. This dependence of amplitude on the rotation rate of the cycloidal turbine is a function of device radius and submergence depth.

Utilizing the study results, an initial model for the steady state frequency response of the cycloidal turbine was developed. This was chosen as a linear time invariant model. The step change results helped to predict model order and damping for this system. This model will be utilized for control development in future efforts involving wave estimation and feedback control. Wave estimation and feedback control algorithms will be essential to operate the cycloidal turbine in the ocean. The step change studies suggest a comprehensive database of wave characteristics in response to changes in cycloidal turbine parameters will need to be created. These recent and past parameter studies of cycloidal turbine radius and submergence show non-linear relationships to the generated wave amplitude. Likewise the steady state generated wave amplitude is a non-linear function of wave generation period. Thus, further test runs will be needed to create a comprehensive database and an algorithm must be developed to determine the best parameters to cancel irregular waves.

In addition to the above tasks for constructing the feedback control algorithm, future work will address issues regarding the device efficiency in irregular waves encountered in the ocean. To explore this, test runs will need to be conducted to determine how effective the feedback control algorithm is in cancelling the irregular waves. Both the accuracy of the wave estimation and performance of the control algorithm will influence this effectiveness. The transients described in the step change runs likewise will affect the effectiveness of wave cancellation and this shortcoming in terms of generating the correct 'anti' will need further investigation. Similarly, the energy that can be extracted from irregular waves will also be studied in future work. With the algorithm controlling the blade pitch angle, device rotation rate, and device submergence in response to changing incoming wave data the flow field at the blade will be continually changing. By knowing the flow field and blade velocities a force and moment analysis can be conducted to determine how much power can be taken by the cycloidal turbine. Using this approach a parameter study of power generation based on the incoming sea state and device parameters such as radius can be conducted. This will help us understand the energy extraction abilities of the cy-

cloidal turbine in addition to the wave cancellation capabilities. Lastly, analysis to include the diffraction due to the disturbance caused by the presence of the device shall be conducted. For the current work, diffraction has been assumed negligible due to the size of the blades relative to the wavelengths considered. This is considered valid because while the blades rotate in large orbits the volume occupied by the device is small. A diffraction code analysis can determine the accuracy of this assumption.

ACKNOWLEDGMENT

We would like to acknowledge the support from our colleagues at the Air Force Academy in particular Mr. Robert Decker of the Modeling and Simulation Center which is led by Dr. Keith Bergeron. This material is based upon activities supported by the National Science Foundation under Agreement No ECCS-0801614. Any opinions, findings, and conclusions or recommendations expressed are those of the authors and do not necessarily reflect the views of the National Science Foundation.

REFERENCES

- [1] Siegel, S.G., 2006. "Cyclical wave energy converter". *pending U.S. and pending/awarded International Patent applications.*
- [2] Hermans, A.J., van Sabben, E., and Pinkster, J.A., 1990. "A device to extract energy from water waves". *Applied Ocean Research Computational Mechanics Publications, Vol.12, No.4*, p.5-9.
- [3] Pinkster, J.A., and Hermans, A.J.. "A rotating wing for the generation of energy from waves". In 22nd IWWF Conference, Plitvice, Croatia.
- [4] Siegel, S.G., Jeans, T., and McLaughlin, T., 2010. "Deep ocean wave energy conversion using a cycloidal turbine". *Applied Ocean Research, submitted.*
- [5] Siegel, S.G., Jeans, T., and McLaughlin, T., 2010. "Intermediate ocean wave termination using a cycloidal wave energy converter". *Proceedings of the 29th International Conference on Ocean, Offshore and Arctic Engineering.* ASME
- [6] Wehausen, J.V. and Laitone, E.V., 1960. *Surface Waves, Handbuch der Physik*, Vol.IX, Springer-Verlag, Berlin, pp. 483-490.
- [7] Boyle, G., 2004. *Renewable Energy - Power for a sustainable future.*, Oxford University Press.